Lubrication flow of a generalized Casson fluid with pressure-dependent rheological paramaters

Lorenzo Fusi[a]

[a]*Dipartimento di Matematica e Informatica "Ulisse Dini"*
Viale Morgagni 67/a, 50134 Firenze, Italy

Abstract

In this paper we model the flow of a generalized Casson fluid in a channel of non uniform amplitude. We assume that the rheological parameters are given functions of the pressure and we suppose that the aspect ratio of the channel is small, so that we can apply the lubrication approximation. We formulate the mathematical problem writing the balance of the linear momentum of the unyielded phase in an integral form. At the leading order of the approximation and when the flow is driven by a given inlet discharge, we may transform the problem is a system of two nonlinear differential equation for the pressure and for the yield surface. When the flow is driven by a given pressure drop the system becomes integro-differential. The solution of the mathematical problem provides the exact location of the yield surface and the velocity field within the channel.

Keywords: Viscoplastic fluid, Casson medium, Lubrication flows,Asymptotic solution

1. Introduction

The viscometric flow of inelastic fluids is commonly modeled by means of constitutive laws of generalized Newtonian fluids, that is fluids in which the shear stress is a function of the shear rate but not dependent on the deformation history. The constitutive response of such fluids allows one to model

*Corresponding author: lorenzo.fusi@unifi.it

many interesting features that are characteristic of non-Newtonian fluids, such as shear-thinning, shear thickening and also yield stress. The simplest generalized Newtonian model is Ostwald-de Waele model (power-law) [18] where the stress is proportional to the rate of shear raised to the power of $n > 0$. When the constitutive response exhibits a yield stress the fluid is called visco-plastic, meaning that a critical value of the stress must be exceeded to start the flow. Among visco-plastic models we mention the Bingham model [2], the Herschel-Bulkley model [12], the Casson model [3] and the Heinz-Casson model [4]. All these models have various practical applications: the Bingham and the Herschel-Bulkley models, for instance, are employed to study flow behavior of muds, foams, ceramics and slurries. The Casson model is widely used to model blood flow, while the Heinz-Casson model is typically employed in the food industry.

In this paper we consider an extension of the Casson model, namely the generalized Casson model. The constitutive response of a generalized Casson fluid is analogous to the one of a Casson fluid with the only difference that the exponent appearing in the constitutive equation can be any positive number $n > 0$ and not necessarily $n = 2$ as in the classical Casson model. The rheological parameters in the constitutive equation of a generalized Casson fluid are the plastic viscosity and the yield stress. Following [7], [10] and [16] we assume that the latter may depend on the pressure.

We model the flow of a generalized Casson fluid in a symmetric channel of varying amplitude under the hypothesis that the characteristic height of the channel is smaller than the length (thin-film flow). We formulate the mathematical problem following the approach introduced in [7] and [8] in which the equation of motion of the unyielded part of the fluid is written in an integral form. This method allows one to predict the correct shape of the yield surface. We remark that the exact form of the yield surface can be determined using other methods that involve higher order terms of thin-film approximation, such as the ones used in [6],[17], [14], [15]. After rescaling the governing equations we focus on the leading order of the lubrication approximation and we determine

an explicit expression for the velocity in terms of the pressure and the the yield surface. The latter are determined using the equation of motion of the unyielded plug and imposing that the unyielded region moves as a rigid body.

When the inlet flow rate is prescribed the problem consists of a system of two nonlinear first order differential equations for the pressure and for the yield surface in which the initial conditions are free parameters that must be selected in order to guarantee the absence of deformations in the unyielded part. When the flow is driven by a given pressure drop between the inlet and the outlet of the channel, the system becomes integro-differential. This result is consistent with what found in [11] in the case of a Herschel-Bulkley fluid.

We initially study the system for constant yield stress and plastic viscosity and we solve the problem for various channel profiles. We find that the behavior of the yield surface is opposite to that of the wall function, meaning that the unyielded core expands when the channel width is reduced and vice versa. This is consistent with the results obtained in [7] and [16] for the Bingham and Herschel-Bulkley model respectively.

Subsequently we consider the case in which the rheological parameters depend on the pressure and solve the problem to investigate the effects that this dependence has on the flow. Besides the increasing complexity of the mathematical problem due to the non constancy of the viscosity and yield stress we find that, differently from the constant case and from the cases studied in [7] and [16], the monotonicity of the yield surface and of the wall function are not necessarily opposite. This means that we can have a reduction of the channel width and of the inner plug at the same time, depending on the particular form of the viscosity and of the yield stress.

A fundamental hypothesis of the present work is that the plug extends continuously from the inlet to the outlet of the channel. This assumption is crucial and our analysis is not applicable when the plug is broken.

2. The mathematical model

We consider a general Casson Fluid whose constitutive equation is given by $\Sigma^* = -p^*\mathbf{I} + \boldsymbol{\tau}^*$ and where the deviatoric part $\boldsymbol{\tau}^*$ is expressed as

$$\begin{cases} \boldsymbol{\tau}^* = \left(\mu^{*\frac{1}{n}} + \dfrac{\tau_y^{*\frac{1}{n}}}{|\dot{\boldsymbol{\gamma}}^*|^{\frac{1}{n}}}\right)^n \dot{\boldsymbol{\gamma}}^*, & |\boldsymbol{\tau}^*| \geqslant \tau_y^*, \\ \\ \dot{\boldsymbol{\gamma}}^* = 0, & |\boldsymbol{\tau}^*| \leqslant \tau_y^*, \end{cases} \tag{1}$$

with $n > 0$ being a real number. Throughout the paper symbols with stars denote dimensional quantities. In (1) μ^* is the plastic viscosity, τ_y^* is the yield stress and

$$\dot{\boldsymbol{\gamma}}^* = \nabla \mathbf{v}^* + \nabla \mathbf{v}^{*^T},$$

is the strain-rate tensor. In the classical generalized Casson model the quantities μ^* and τ_y^* are positive constants. Here we assume that the viscosity and the yield stress are positive known functions of the pressure, i.e.

$$\mu^* = \mu_o^* \mu\Big(\alpha^*(p^* - p_o^*)\Big), \qquad \tau_y^* = \tau_o^* \tau_y\Big(\beta^*(p^* - p_o^*)\Big). \tag{2}$$

In (2) the functions μ and τ_y are positive and such that $\mu(0) = \tau_y(0) = 1$, while μ_o^* and τ_o^* are the viscosity and the yield stress at the reference pressure p_o^*. The quantities

$$|\boldsymbol{\tau}^*| = \sqrt{\frac{1}{2}\boldsymbol{\tau}^* \cdot \boldsymbol{\tau}^*}, \qquad |\dot{\boldsymbol{\gamma}}^*| = \sqrt{\frac{1}{2}\dot{\boldsymbol{\gamma}}^* \cdot \dot{\boldsymbol{\gamma}}^*},$$

represent the norm of the deviatoric stress $\boldsymbol{\tau}^*$ and the norm of the strain-rate $\dot{\boldsymbol{\gamma}}^*$ respectively. The stress-strain relation can be represented in a Cartesian plot taking the norm of $(1)_1$, namely

$$|\boldsymbol{\tau}^*| = \left[\Big(\mu^*|\dot{\boldsymbol{\gamma}}^*|\Big)^{\frac{1}{n}} + \tau_y^{*\frac{1}{n}}\right]^n. \tag{3}$$

Setting

$$\eta = \left|\frac{\boldsymbol{\tau}^*}{\tau_y^*}\right|, \qquad \xi = \left(\frac{\mu^*|\dot{\boldsymbol{\gamma}}^*|}{\tau_y^*}\right),$$

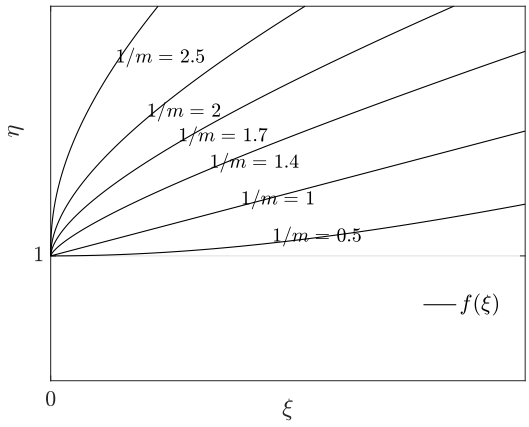

Figure 1: The function $\eta = f(\xi)$ for different values of n.

the stress strain relation can be investigated through the function

$$\eta = f(\xi) = \left(1 + \xi^{\frac{1}{n}}\right)^n : \mathbb{R}^+ \cup \{0\} \longrightarrow \mathbb{R}^+ \cup \{0\}. \tag{4}$$

as shown in Fig. 1. We observe that $f(\xi) \to \infty$ for $\xi \to \infty$ and that $f(\xi)$ has an oblique asymptote for $\xi \to \infty$ only if $0 < n \leqslant 1$. More precisely, the asymptote oblique is

$$\begin{cases} \eta = \xi, & n \in (0,1), \\ \\ \eta = 1 + \xi, & n = 1. \end{cases}$$

For ξ sufficiently large and $n \in (0,1)$, we have that $f(\xi) \sim \xi$ and (3) becomes

$$|\boldsymbol{\tau}^*| = \mu^* |\dot{\boldsymbol{\gamma}}^*|, \qquad |\dot{\boldsymbol{\gamma}}^*| \gg 1, \tag{5}$$

while, for ξ sufficiently large and $n = 1$

$$|\boldsymbol{\tau}^*| = \mu^* |\dot{\boldsymbol{\gamma}}^*| + \tau_y^*, \qquad |\dot{\boldsymbol{\gamma}}^*| \geqslant 0. \tag{6}$$

When $n = 1$ we recover the Bingham model with pressure dependent rheological moduli, while for $n = 2$ we obtain the Casson model with pressure dependent rheological moduli. In our model we simply assume that $n > 0$, i.e. we consider a generalized Casson model with pressure-dependent yield stress and viscosity.

Let us consider the flow in a symmetric channel of length L^* whose walls are expressed by $y^* = \pm h^*(x^*)$. The velocity field is given by

$$\mathbf{v}^*(x^*, y^*, t^*) = u^*(x^*, y^*, t^*)\mathbf{e}_1 + v^*(x^*, y^*, t^*)\mathbf{e}_2.$$

The flow domain is dividend in a yielded region

$$\Omega_y^*(t^*) = \Big\{(x^*, y^*) : x^* \in [0, L^*], \quad y^* \in [-h^*, -\sigma^*] \cup [\sigma^*, h^*]\Big\},$$

and an unyielded region

$$\Omega_u^*(t) = \Big\{(x^*, y^*) : x^* \in [0, L^*], \quad y^* \in [-\sigma^*, \sigma^*]\Big\},$$

where $y^* = \pm\sigma^*(x^*, t^*)$ represent the yield surfaces. Within $\Omega_u^*(t^*)$ the fluid is unyielded and $|\boldsymbol{\tau}^*| \leqslant \tau_y^*$ while in $\Omega_y^*(t^*)$ the fluid is yielded and we have $|\boldsymbol{\tau}^*| \geqslant \tau_y^*$. Notice that both $\Omega_u^*(t^*)$ and $\Omega_y^*(t^*)$ are not material volumes. We make the assumption that the core extends from the inlet to the outlet, so that the rigid plug never breaks. Assuming incompressibility and neglecting the body forces, the governing equations of the system are

$$\operatorname{div} \mathbf{v}^* = 0 \qquad (x^*, y^*) \in \Omega_u^*(t^*) \cup \Omega_y^*(t^*), \tag{7}$$

$$\rho^* \dot{\mathbf{v}}^* = -\nabla p^* + \operatorname{div}(\boldsymbol{\tau}^*) \qquad (x^*, y^*) \in \Omega_y^*(t^*), \tag{8}$$

$$\int\limits_{\Omega_u^*(t^*)} \rho^* \dot{\mathbf{v}}^* dV^* = \int\limits_{\partial\Omega_u^*(t^*)} \boldsymbol{\sigma}^* \mathbf{n} dS^*. \tag{9}$$

where the dot means material differentiation. The balance of linear momentum in $\Omega_u^*(t^*)$ is written in the integral form (9) because the body is undeformable in the unyielded domain (the continuum behaves as rigid body below the yield limit) and hence the stress is undetermined, see [5]. Boundaries of the plug region are located via the yield criterion

$$|\boldsymbol{\tau}^*|\Big|_{y^* = \pm\sigma^*} = \tau_y^*, \tag{10}$$

that, recalling (3), can be written also as

$$|\dot{\boldsymbol{\gamma}}^*|\Big|_{y^*=\pm\sigma^*} = 0. \tag{11}$$

We assume the continuity of the stress and velocity across $y^* = \pm\sigma^*$ and impose the no-slip conditions $\mathbf{v}^* = 0$ on $y^* = \pm h^*$. We notice that, because of symmetry, the velocity in $\Omega_u^*(t^*)$ is given by $\mathbf{v}_c^*(t^*) = u_c^*(t^*)\mathbf{e}_1$. Following the approach of [9], we limit our analysis to the upper part of the channel $y^* \geqslant 0$ and we write the governing equations component-wise as

$$u^*_{x^*} + v^*_{y^*} = 0, \tag{12}$$

$$\rho^* \left(u^*_{t^*} + u^*_{x^*} u^* + u^*_{y^*} v^* \right) = -p^*_{x^*} + (\tau^*_{11})_{x^*} + (\tau^*_{12})_{y^*}, \tag{13}$$

$$\rho^* \left(v^*_{t^*} + v^*_{x^*} u^* + v^*_{y^*} v^* \right) = -p^*_{y^*} + (\tau^*_{12})_{x^*} + (\tau^*_{22})_{y^*}, \tag{14}$$

$$\rho^* \dot{u}^*_c \int_0^{L^*} \sigma^* dx^* = \int_0^{L^*} \Big(-\sigma^* p^*_x - \sigma^*_x \tau^*_{11} + \tau^*_{12} \Big)\Big|_{\sigma^*} dx^*. \tag{15}$$

We remark that the last equation represents the first component of the balance equation (9) since the second is automatically satisfied if one assumes that on the lateral surfaces $x^* = 0$, $x^* = L^*$ the tangential stresses are zero (no torque is applied on the rigid plug). We rescale the problem as follows

$$x^* = L^* x, \qquad y^* = H^* y, \qquad t^* = \left(\frac{L^*}{U^*} \right) t,$$

$$u^* = U^* u, \qquad v^* = \epsilon U^* v, \qquad u^*_c = U u_c,$$

$$h^* = H^* h, \qquad \sigma^* = H^* \sigma, \qquad \boldsymbol{\tau}^* = \left(\frac{\mu^*_o U^*}{H^*} \right) \boldsymbol{\tau},$$

$$\dot{\boldsymbol{\gamma}}^* = \left(\frac{U^*}{H^*} \right) \dot{\boldsymbol{\gamma}}, \qquad p^* - p^*_o = \left(\frac{\mu^*_o U^* L^*}{H^{*^2}} \right) p,$$

$$\alpha^* = \left(\frac{{H^*}^2}{\mu_o^* U^* L^*}\right)\alpha, \qquad \beta^* = \left(\frac{{H^*}^2}{\mu_o^* U^* L^*}\right)\beta,$$

where L^* is the length of the channel and $H^* = \max_{[0,L^*]} h^*(x^*)$. We make the assumption of small aspect ratio

$$\epsilon = \frac{H^*}{L^*} \ll 1.$$

Following [16], without loss of generality we assume that $p_o^* = p_{out}^*$, where p_{out}^* is the constant pressure at the outlet of the channel. Hence the non dimensional inlet pressure becomes

$$p\Big|_{x=0} = \Delta p = \frac{\Delta p^*}{\left(\frac{\mu_o^* U^* L^*}{{H^*}^2}\right)} = \frac{p_{in}^* - p_{out}^*}{\left(\frac{\mu_o^* U^* L^*}{{H^*}^2}\right)}, \tag{16}$$

while the non dimensional outlet pressure is identically zero. Equations (12)-(15) become

$$u_x + v_y = 0, \tag{17}$$

$$\epsilon Re\,(u_t + u_x u + u_y v) = -p_x + \epsilon(\tau_{11})_x + (\tau_{12})_y, \tag{18}$$

$$\epsilon^3 Re\,(v_t + v_x u + v_y v) = -p_y + \epsilon^2(\tau_{12})_x + (\tau_{22})_y, \tag{19}$$

$$\epsilon Re \dot{u}_c \int_0^1 \sigma dx = \int_0^1 \left[-p_x\sigma - \epsilon\sigma_x\tau_{11} + \tau_{12}\right]\big|_\sigma \, dx, \tag{20}$$

where

$$Re = \left(\frac{\rho^* U^* H^*}{\mu_o^*}\right)$$

is the Reynolds number. The non dimensional stress becomes

$$\boldsymbol{\tau} = \left[\mu(\alpha p)^{\frac{1}{n}} + \frac{\left(B\tau_y(\beta p)\right)^{\frac{1}{n}}}{|\dot{\bar{\boldsymbol{\gamma}}}|^{\frac{1}{n}}}\right]^n \dot{\boldsymbol{\gamma}},$$

where

$$B = \left(\frac{\tau_o^* H^*}{\mu_o^* U^*}\right),$$

is the Bingham number. The non-dimensional strain rate norm is

$$|\dot{\boldsymbol{\gamma}}| = \sqrt{2\epsilon^2\left(u_x^2 + v_y^2\right) + \left(u_y + \epsilon^2 v_x\right)^2}. \tag{21}$$

The yield criterion is given by

$$|\boldsymbol{\tau}|\Big|_\sigma = B\tau_y(\beta p) \qquad \longleftrightarrow \qquad |\dot{\boldsymbol{\gamma}}|\Big|_\sigma = 0.$$

3. Zero order problem

We focus on the leading order approximation assuming that Re, $B = O(1)$. Neglecting all the terms containing ϵ we get

$$\begin{cases} u_x + v_y = 0, \\ (\tau_{12})_y = p_x, \qquad \text{(Yielded phase)} \quad y \in [\sigma, h], \\ p_y = 0, \end{cases} \tag{22}$$

$$\begin{cases} \displaystyle\int_0^1 \left(-p_x\sigma + \tau_{12}\right)\big|_\sigma \, dx = 0, \\ \qquad\qquad\qquad\qquad \text{(Unyielded phase)} \quad y \in [0, \sigma], \\ u = u_c, \qquad v = 0, \end{cases} \tag{23}$$

where

$$\tau_{12} = u_y \left[\mu(\alpha p)^{\frac{1}{n}} + \frac{\Big(B\tau_y(\beta p)\Big)^{\frac{1}{n}}}{|u_y|^{\frac{1}{n}}} \right]^n.$$

On the yield surface

$$\Big|\dot{\boldsymbol{\gamma}}\Big|_\sigma = |u_y|_\sigma = 0.$$

In the upper yielded part $u_y < 0$. Therefore

$$\tau_{12} = -\left[\left(\mu(\alpha p)\,|u_y|\right)^{\frac{1}{n}} + \Big(B\tau_y(\beta p)\Big)^{\frac{1}{n}} \right]^n, \tag{24}$$

and the yield condition becomes

$$\tau_{12}\Big|_\sigma = -\Big(B\tau_y(\beta p)\Big).$$

From $(22)_3$ we see that $p = p(x,t)$ so that, integrating $(22)_2$ between σ and y we find

$$\tau_{12} = -B\tau_y(\beta p) + p_x(y-\sigma). \tag{25}$$

Subtracting (24) from (25) we find

$$u_y = -\left(\frac{B\tau_y(\beta p)}{\mu(\alpha p)}\right)\left[\left(1+\frac{p_x}{B\tau_y(\beta p)}(\sigma-y)\right)^{\frac{1}{n}}-1\right]^n. \tag{26}$$

Assuming that the pressure drop $\Delta p > 0$ we expect $p_x < 0$ and $p_x(\sigma - y) > 0$ in the yielded phase, so that (26) is well defined for every $n > 0$. We define

$$\mathcal{P} = \int \frac{dp}{B\tau_y(\beta p)}, \qquad \longrightarrow \qquad \mathcal{P}_x = \frac{p_x}{B\tau_y(\beta p)},$$

and we integrate (26) between y and h exploiting the no-slip condition getting

$$\frac{u}{B} = g(p)\int_y^h \left[(1+\mathcal{P}_x(\sigma-\xi))^{\frac{1}{n}}-1\right]^n d\xi, \tag{27}$$

where for simplicity we have set

$$g(p) = \frac{\tau_y(\beta p)}{\mu(\alpha p)}. \tag{28}$$

The velocity of the core is thus

$$\frac{u_c}{B} = g(p)\int_\sigma^h \left[(1+\mathcal{P}_x(\sigma-\xi))^{\frac{1}{n}}-1\right]^n d\xi. \tag{29}$$

Subtracting (29) from (27) we find

$$\frac{u}{u_c} = 1 - \frac{\displaystyle\int_\sigma^y \left[(1+\mathcal{P}_x(\sigma-\xi))^{\frac{1}{n}}-1\right]^n d\xi}{\displaystyle\int_\sigma^h \left[(1+\mathcal{P}_x(\sigma-\xi))^{\frac{1}{n}}-1\right]^n d\xi}. \tag{30}$$

Exploiting the mass balance $u_x = -v_y$ we write

$$v = \int_\sigma^y v_y dy = -\int_\sigma^y u_x dy,$$

that is

$$v = u_c \int_\sigma^y \frac{d}{dx} \left[\frac{\int_\sigma^{\tilde{y}} \left[(1 + \mathcal{P}_x(\sigma - \xi))^{\frac{1}{n}} - 1 \right]^n d\xi}{\underbrace{\int_\sigma^h \left[(1 + \mathcal{P}_x(\sigma - \xi))^{\frac{1}{n}} - 1 \right]^n d\xi}_{=u_c/(Bg(p))}} \right] d\tilde{y}.$$

Recalling that u_c does not depend on x and y we find

$$v = B \int_\sigma^y \frac{d}{dx} \left[\int_\sigma^{\tilde{y}} g(p) \left[(1 + \mathcal{P}_x(\sigma - \xi))^{\frac{1}{n}} - 1 \right]^n d\xi \right] d\tilde{y},$$

or equivalently

$$v = B \int_\sigma^y d\tilde{y} \int_\sigma^{\tilde{y}} \frac{d}{dx} \left[g(p) \left[(1 + \mathcal{P}_x(\sigma - \xi))^{\frac{1}{n}} - 1 \right]^n \right] d\xi d\tilde{y}. \tag{31}$$

Exploiting again the mass balance we see that

$$\frac{d}{dx} \left(\int_\sigma^h u dy \right) = -u_c \sigma_x + \underbrace{\left(\int_\sigma^h u_x dy \right)}_{=0},$$

implying

$$\frac{d}{dx} \left(\int_\sigma^h \frac{u}{u_c} dy + \sigma \right) = 0. \tag{32}$$

In conclusion we find that

$$\int_\sigma^h \frac{u}{u_c} dy + \sigma = Q, \tag{33}$$

where $Q > 0$ is a constant representing the non dimensional discharge on a generic cross section x of the channel normalized with the core velocity u_c. Inserting (30) into (33) we get

$$h - \frac{\int_\sigma^h dy \int_\sigma^y \left[(1 + \mathcal{P}_x(\sigma - \xi))^{\frac{1}{n}} - 1 \right]^n d\xi}{\int_\sigma^h \left[(1 + \mathcal{P}_x(\sigma - \xi))^{\frac{1}{n}} - 1 \right]^n d\xi} = Q. \tag{34}$$

The core equation $(23)_1$ becomes

$$\int_0^1 \Big[- p_x\sigma - B\tau_y(\beta p)\Big]dx = 0,$$

and can be rewritten as

$$\int_0^1 \left[1 + \mathcal{P}_x\sigma\right]\tau_y(\beta p)dx = 0. \tag{35}$$

Finally, recalling that u_c must be independent of x and recalling (29), we write

$$\frac{d}{dx}\left[g(p)\int_\sigma^h \left[(1+\mathcal{P}_x(\sigma-\xi))^{\frac{1}{n}} - 1\right]^n d\xi\right] = 0. \tag{36}$$

Equations (34), (35),(36) provide the mathematical formulation of the problem. In order to have a lighter notation we introduce the new variable

$$z = \mathcal{P}_x(\sigma - h) > 0.$$

It is easy to show that with this substitution equations (34), (35),(36) become

$$\frac{1}{\mathcal{P}_x}\frac{\displaystyle\int_1^{1+z} dy \int_1^y \left[\zeta^{\frac{1}{n}} - 1\right]^n d\zeta}{\displaystyle\int_1^{1+z} \left[\zeta^{\frac{1}{n}} - 1\right]^n d\zeta} = Q - h, \tag{37}$$

$$\int_0^1 \left[1 + z + \mathcal{P}_x h\right]\tau_y(\beta p)dx = 0, \tag{38}$$

$$\frac{d}{dx}\left[\frac{g(p)}{\mathcal{P}_x}\int_1^{1+z} \left[\zeta^{\frac{1}{n}} - 1\right]^n d\zeta\right] = 0. \tag{39}$$

Now we introduce the functions

$$N(z) = \int_1^{1+z} dy \int_1^y \left[\zeta^{\frac{1}{n}} - 1\right]^n d\zeta, \tag{40}$$

$$D(z) = \int_1^{1+z} \left[\zeta^{\frac{1}{n}} - 1\right]^n d\zeta, \tag{41}$$

and we note that $N'(z) = D(z)$. The system (37), (38),(39) can be rewritten as

$$\begin{cases} p_x = \dfrac{BN(z)\tau_y(\beta p)}{D(z)(Q-h)}, \\ \\ \displaystyle\int_0^1 \left[1 + z + \frac{N(z)h}{D(z)(Q-h)}\right] \tau_y(\beta p)dx = 0, \\ \\ \dfrac{d}{dx}\left[\dfrac{g(p)(Q-h)D(z)^2}{N(z)}\right] = 0. \end{cases} \tag{42}$$

Now, differentiating the last expression we find

$$g'(p)p_x\frac{(Q-h)D^2}{N}+$$

$$+g(p)\left[\frac{-h_xD^2N + z_x(Q-h)D(2D'N - N'D)}{N^2}\right] = 0.$$

Recalling $(42)_1$, the above can be rewritten as

$$z_x = \frac{h_xD(z)N(z) - Bg'(p)g^{-1}(p)\tau_y(\beta p)N^2(z)}{(Q-h)(2D'(z)N(z) - D^2(z))}.$$

Suppose that the inlet flux Q is given. Then we must solve the system

$$\begin{cases} p_x = \dfrac{BN\tau_y(\beta p)}{D(Q-h)}, & p\Big|_{x=0} = p_o, \\ \\ z_x = \dfrac{h_xDN - g'g^{-1}B\tau_yN^2}{(Q-h)(2D'N - D^2)}, & z\Big|_{x=0} = z_o, \end{cases} \tag{43}$$

where z_o and p_o are pivotable parameters at this stage. The equation for the plug is

$$\int_0^1 \left[1 + z + \frac{N(z)h}{D(z)(Q-h)}\right] \tau_y(\beta p)dx = 0, \tag{44}$$

and can be rewritten as

$$\int_0^1 \left[B(1+z)\tau_y(\beta p) + p_xh\right] dx = 0. \tag{45}$$

Now, from $(43)_1$, we see that

$$p_xh = p_xQ - \frac{BN(z)\tau_y(\beta p)}{D(z)},$$

which, once inserted into (45), provides

$$Q = \frac{B}{\Delta p} \int_0^1 \left(1 + z - \frac{N(z)}{D(z)}\right) \tau_y(\beta p) dx. \tag{46}$$

To determine the parameters z_o and p_o we proceed in the following way. The solution of (43) is given by the functions

$$z = z(x; z_o, p_o), \qquad\qquad p = p(x; z_o, p_o), \tag{47}$$

that depend on the choice of the inlet conditions z_o and p_o. The functions p and z must satisfy equations (45) and (46). Recalling that $p|_{x=0} = p_o = \Delta p$ we must therefore choose p_o and z_o such that the system

$$\begin{cases} \displaystyle\int_0^1 \left[B(1+z)\tau_y(\beta p) + p_x h\right] dx = 0, \\ \\ \displaystyle\int_0^1 \left(1 + z - \frac{N(z)}{D(z)}\right) \tau_y(\beta p) dx - \frac{Q p_o}{B} = 0, \end{cases} \tag{48}$$

is satisfied. Indeed, from (47), it is clear that (48) is a nonlinear algebraic system for the unknowns p_o and z_o. When Δp is given, then Q is given by (46) and the system (43) becomes integro-differential with the initial conditions that must be chosen in order to satisfy (44). Once the problem (43), (48) is solved σ can be evaluated noticing that

$$\mathcal{P}_x = \frac{z}{\sigma - h} = \frac{N(z)}{D(z)(Q - h)},$$

which implies

$$\sigma = h\left(1 - \frac{zD(z)}{N(z)}\right) + \frac{zD(z)}{N(z)} Q. \tag{49}$$

3.1. Flow conditions

We can easily prove that

$$\lim_{z\to 0} \frac{zD(z)}{N(z)} = 2 + n, \qquad\qquad \lim_{z\to\infty} \frac{zD(z)}{N(z)} = 3$$

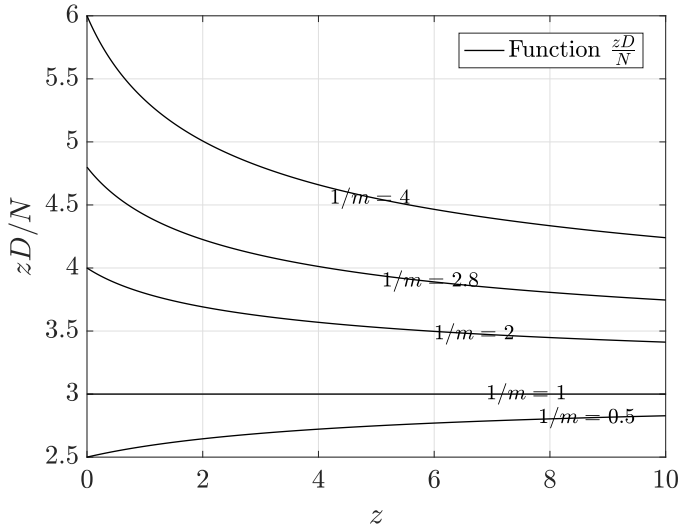

Figure 2: The function zD/N.

and

$$\begin{cases} 3 < \dfrac{zD(z)}{N(z)} < 2+n, & n > 1, \\ \\ 3 = \dfrac{zD(z)}{N(z)}, & n = 1, \\ \\ 2+n < \dfrac{zD(z)}{N(z)} < 3, & n < 1, \end{cases} \tag{50}$$

as shown in Fig. 2. Following (49) we see that the condition $\sigma \in (0,1)$ is guaranteed if

$$h\underbrace{\left(1-\frac{N(z)}{zD(z)}\right)}_{>0 \quad \forall n} < Q < \frac{N(z)}{zD(z)} + h\left(1-\frac{N(z)}{zD(z)}\right),$$

or equivalently if

$$\frac{h\left(1-\dfrac{N(z)}{zD(z)}\right)}{\displaystyle\int_0^1 \underbrace{\left(1+z-\frac{N(z)}{D(z)}\right)}_{>0 \quad \forall n} \tau_y(\beta p)dx} < \frac{B}{\Delta p} < \frac{\dfrac{N(z)}{zD(z)} + h\left(1-\dfrac{N(z)}{zD(z)}\right)}{\displaystyle\int_0^1 \left(1+z-\frac{N(z)}{D(z)}\right)\tau_y(\beta p)dx}.$$

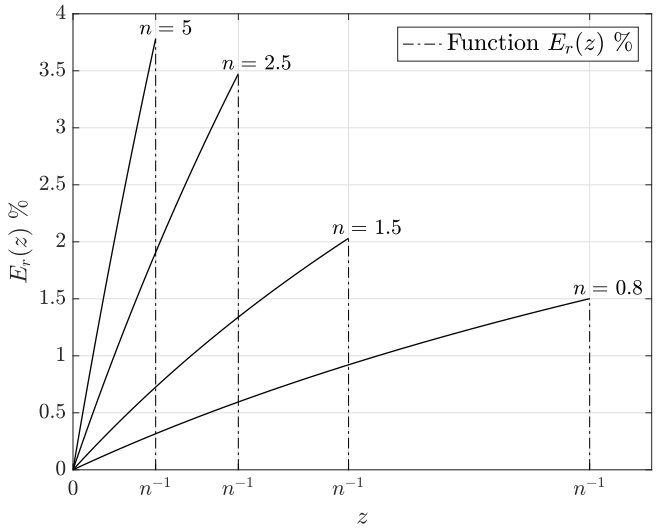

Figure 3: The function $E_r(z)$.

When $n = 1$

$$\frac{zD(z)}{N(z)} = 3,$$

so that

$$\sigma = -2h + 3Q \qquad \longrightarrow \qquad \sigma_x = -2h_x,$$

consistently with the expression for σ obtained in [7] for a Bingham fluid.

3.2. Approximated solution

We notice that for $z \leqslant 1/n$ the function $zD(z)/N(z)$ can be safely approximated by the constant $(n + 2)$. Indeed let us consider the function

$$E_r(z) = 100 \cdot \left| 1 - \frac{zD(z)/N(z)}{n+2} \right| \ \%, \tag{51}$$

that provides the relative error made when one approximates the function $zD(z)/N(z)$ with $(n + 2)$. As one can see from the plots in Fig. 3 this error is less than 5% when $z \leqslant (1/n)$ and for $n = 1$ the error is identically null. Therefore, if $z \leqslant 1/n$ we may approximate σ with

$$\sigma = -h(1 + n) + (n + 2)Q,$$

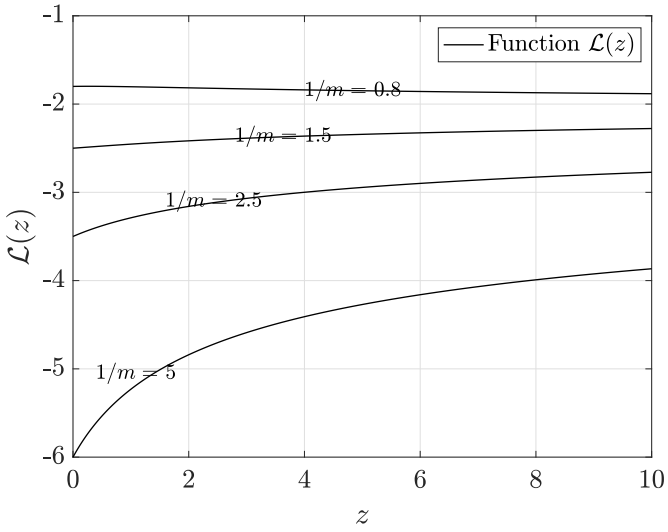

Figure 4: The function $\mathcal{L}(z)$.

so that

$$\sigma_x = -h_x(1+n).$$

The above relation shows that the monotonicity of the yield surface is opposite to the one of the wall. This behavior is visible in the numerical simulations of the next section.

4. Constant rheological parameters

When $\tau_y = \mu = g = 1$ the constitutive moduli are constant and the system (43) simplifies to

$$\begin{cases} p_x = \dfrac{BN}{D(Q-h)}, & p\Big|_{x=0} = p_o, \\ \\ z_x = \dfrac{h_x DN}{(Q-h)(2D'N - D^2)}, & z\Big|_{x=0} = z_o, \end{cases} \tag{52}$$

and

$$\int_0^1 \left[1 + z + \frac{N(z)h}{D(z)(Q-h)}\right] dx = 0. \tag{53}$$

In this case equation $(52)_2$ becomes independent of p and so does the integral equation (53). Therefore we can solve the problem $(52)_2$ for z and we adjust the parameter z_o to satisfy (53). Once the solution is found we evaluate the pressure through $(52)_1$ adjusting the parameter $p_o = \Delta p$ so that

$$Q = \frac{B}{\Delta p} \int_0^1 \left(1 + z - \frac{N(z)}{D(z)}\right) dx, \tag{54}$$

is satisfied. From (49) we notice that

$$\sigma_x = h_x \left(1 - \frac{zD}{N}\right) + \frac{d}{dz}\left(\frac{zD}{N}\right)(Q - h) z_x.$$

Substituting z_x with $(52)_2$ in the relation above we find

$$\sigma_x = h_x \left[1 - \frac{zD}{N} + \frac{D}{N}\left(\frac{zD'N - zD^2 + DN}{2D'N - D^2}\right)\right].$$

After some extra algebra we get

$$\sigma_x = h_x \left(\frac{2D'N - zD'D}{2D'N - D^2}\right) = h_x \mathcal{L}(z).$$

The function $\mathcal{L}(z)$ is strictly negative for $z \geqslant 0$ for all $n > 0$, as shown in Fig. 4. This proves that, in the case of constant rheological parameters, the wall and the yield surface have opposite monotonicity and $\sigma_x = 0$ whenever $h_x = 0$. Moreover, recalling the expression for the transversal velocity (31), we see that in the case of constant viscosity and yield stress the transversal velocity can be rewritten as

$$v = \frac{\partial}{\partial x}\left[\frac{B}{\mathcal{P}_x^2} \int_1^{1+\mathcal{P}_x(\sigma - y)} d\tilde{y} \int_1^{\tilde{y}} (\zeta^{\frac{1}{n}} - 1)^n d\zeta\right]$$

Now recall that $\mathcal{P}_x(\sigma - h) = z$ so that

$$v = \frac{\partial}{\partial x} \underbrace{\left[\frac{B(\sigma - h)^2}{z^2} \int_1^{1+z\left(\frac{\sigma - y}{\sigma - h}\right)} d\tilde{y} \int_1^{\tilde{y}} (\zeta^{\frac{1}{n}} - 1)^n d\zeta\right]}_{\mathcal{F}(z, \sigma, h; y)},$$

and

$$v = \frac{\partial}{\partial x}\Big[\mathcal{F}(z, \sigma, h; y)\Big] = \frac{\partial \mathcal{F}}{\partial z} z_x + \frac{\partial \mathcal{F}}{\partial \sigma} \sigma_x + \frac{\partial \mathcal{F}}{\partial h} h_x. \tag{55}$$

When $h_x = 0$ we get $z_x = \sigma_x = 0$ and the transversal velocity v is identically zero whenever $h_x = 0$, as we shall see from the numerical simulations.

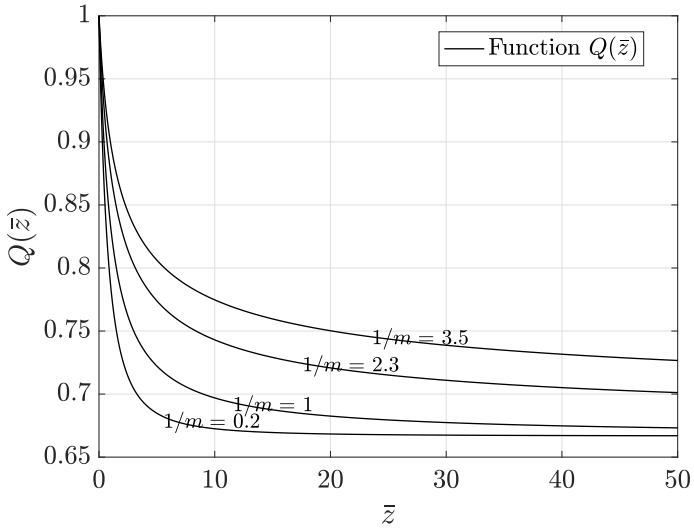

Figure 5: The function $Q(\bar{z})$ for $n = 0.2, 1, 2.3, 3.5$.

4.1. Flat channel

When $h = 1$ we find that $z_x = 0$ and $z = \bar{z} = const.$ From (53)

$$Q = Q(\bar{z}) = 1 - \frac{1}{1+\bar{z}} \frac{N(\bar{z})}{D(\bar{z})}.$$

It is easy to prove that

$$\lim_{\bar{z}\to 0} Q(\bar{z}) = 1, \qquad \lim_{\bar{z}\to\infty} Q(\bar{z}) = \frac{2}{3}, \qquad \frac{dQ(\bar{z})}{d\bar{z}} < 0,$$

for all $n > 0$, as shown in Fig. 5 Therefore we determine a unique solution $\bar{z}$ only if we impose a discharge $Q \in (2/3, 1)$. Moreover, since we want $\bar{z} = O(1)$ we must ensure that the selected Q provides a $\bar{z} = O(1)$. Looking at Fig. 5 we realize that for large values of n the imposed flux Q must be close to one in order to guarantee that $\bar{z} = O(1)$. On the other hand, if Δp is given instead of Q from (54) we have

$$\frac{B}{\Delta p}\left(1 + \bar{z} - \frac{N(\bar{z})}{D(\bar{z})}\right) = \left(1 - \frac{1}{1+\bar{z}} \frac{N(\bar{z})}{D(\bar{z})}\right), \tag{56}$$

so that

$$\bar{z} = \frac{\Delta p}{B} - 1, \tag{57}$$

for all $n > 0$. In this case the solution has a physical meaning only if $\bar{z} > 0$, that is if $\Delta p > B$. This proves that in a flat channel with constant yield stress and viscosity the flow condition for a generalized Casson fluid is exactly the one of a classical Bingham fluid, see [13].

4.2. Case 1: n integer

When n is integer the functions $N(z)$ and $D(z)$ can be evaluated through the binomial theorem

$$(\zeta^{\frac{1}{n}} - 1)^n = \sum_{k=0}^{n} \begin{pmatrix} n \\ k \end{pmatrix} (-1)^k \zeta^{1-\frac{k}{n}}.$$

Inserting the above into (40), (41) and calculating the integrals we find

$$N(z) = \sum_{k=0}^{n} a_{nk} \left[\frac{\left(1+z\right)^{3-\frac{k}{n}} - z\left(3-\frac{k}{n}\right) - 1}{\left(2-\frac{k}{n}\right)\left(3-\frac{k}{n}\right)} \right], \tag{58}$$

$$D(z) = \sum_{k=0}^{n} a_{nk} \left[\frac{\left(1+z\right)^{2-\frac{k}{n}} - 1}{\left(2-\frac{k}{n}\right)} \right]. \tag{59}$$

When $n = 1$ we retrieve the Bingham model studied in [7]. Indeed in this case it is easy to verify that

$$\begin{cases} p_x = \dfrac{Bz}{3(Q-h)}, & p\Big|_{x=0} = p_o, \\ \\ z_x = \dfrac{h_x z}{(Q-h)}, & z\Big|_{x=0} = z_o, \end{cases} \tag{60}$$

and

$$Q = \frac{B}{\Delta p} \int_0^1 \left(1 + \frac{2z}{3}\right) dx. \tag{61}$$

Recalling that $Bz = p_x(\sigma - h)$ from $(60)_1$ we easily check that $(\sigma - h) = 3(Q-h)$ and $(\sigma_x - h_x) = -3h_x$. Hence

$$z = \frac{3p_x}{B}(Q-h),$$

which inserted into (61) yields

$$3Q = \frac{1}{\Delta p}\left[B - 2\int_0^1 p_x h dx\right]. \tag{62}$$

Finally, we observe that

$$\frac{p_x}{z_x} = \frac{B}{3h_x}, \qquad \longrightarrow \qquad p_{xx}(\sigma - h) + p_x(\sigma_x - h_x) = 3p_x h_x,$$

leading to

$$p_{xx} + \frac{6h_x}{\left[3h + \frac{1}{\Delta p}\left(2\int_0^1 p_x h dx - B\right)\right]} = 0, \tag{63}$$

which is exactly the integro-differential euqation for the pressure that has been determined in [7].

4.3. Numerical examples

Here we perform some numerical simulations in the case of constant rheological parameters. We investigate the behavior of the yield surface and of the velocity field for some values of the parameters of the model. We consider three different situations: i) convergent channel; ii) divergent channel; iii) non monotonic channel. For each case we plot the velocity components and the yield surface. In Table 1, 2, 3 we indicate the values of the parameters and the channel profiles for each case.

Channel profile	Q	B	n	z_o	Figure
$h(x) = 1 - 0.1x^2$	0.78	2	0.5	0.636	Fig. 6, 7
$h(x) = 1 - 0.1x^2$	0.78	10	2.0	1.9	Fig. 8, 9

Table 1: Case i) Convergent channel.

As proved earlier the spatial derivative of the yield surface and of the wall function have opposite sign. For simplicity we consider only the case in which the flow is driven imposing a given volumetric flow rate Q at the inlet. In the

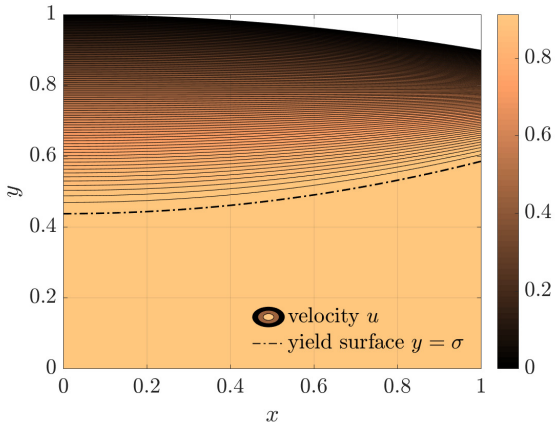

Figure 6: Case i) $n = 0.5$. Velocity component u.

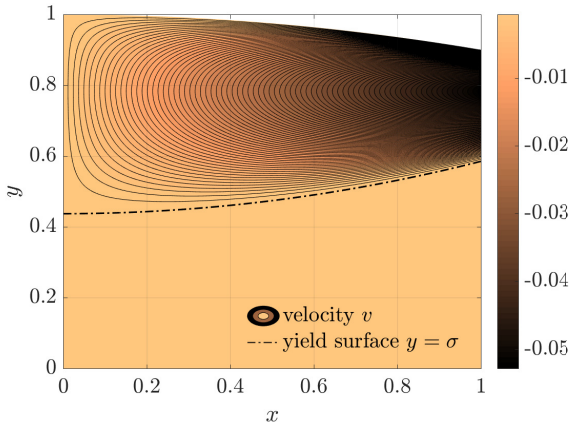

Figure 7: Case i) $n = 0.5$. Velocity component v.

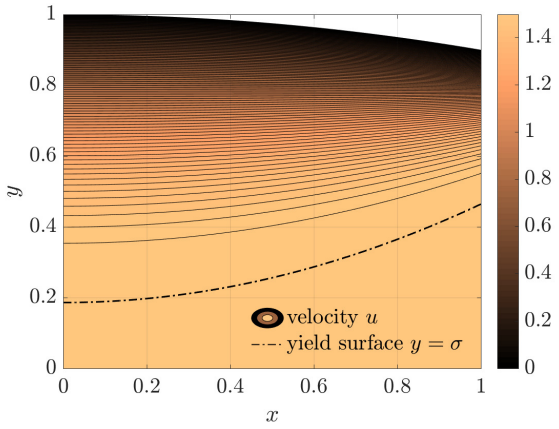

Figure 8: Case i) $n = 2$. Velocity component u.

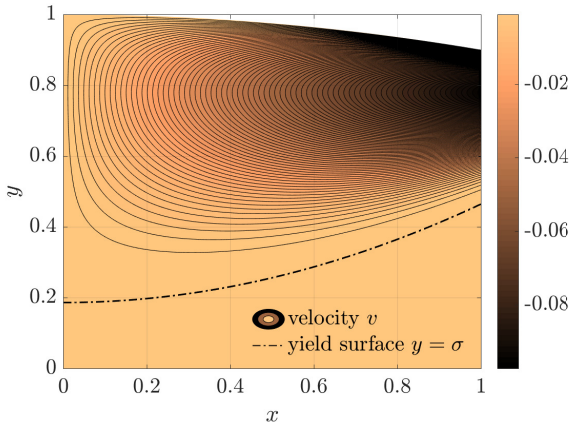

Figure 9: Case i) $n = 2$. Velocity component v.

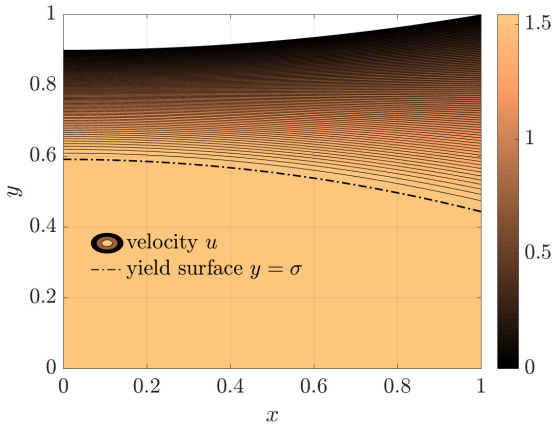

Figure 10: Case ii) $n = 0.5$. Velocity component u.

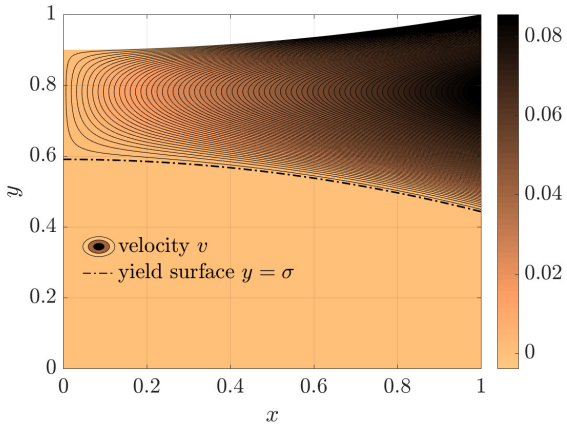

Figure 11: Case ii) $n = 0.5$. Velocity component v.

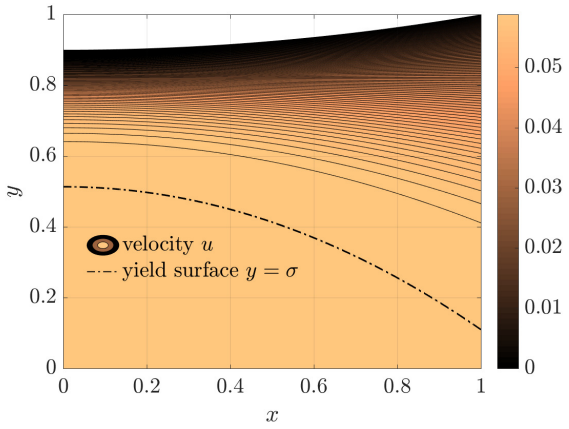

Figure 12: Case ii) $n = 3.5$. Velocity component u.

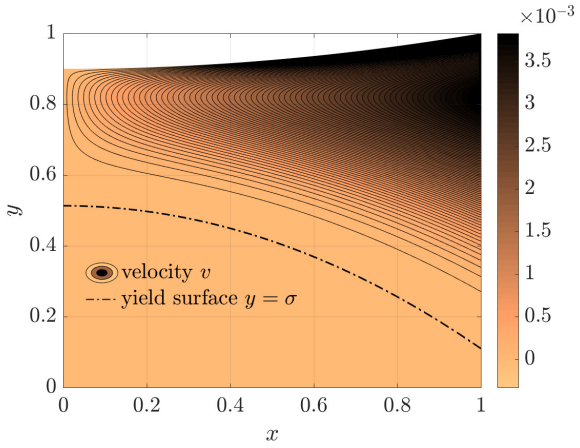

Figure 13: Case ii) $n = 3.5$. Velocity component v.

Channel profile	Q	B	n	z_o	Figure
$h(x) = 0.9 + 0.1x^2$	0.78	5	0.5	0.904	Fig. 10, 11
$h(x) = 0.9 + 0.1x^2$	0.82	10	3.5	1.37	Fig. 12, 13

Table 2: Case ii) Divergent channel.

case of a converging channel i) we observe that an increase of the Bingham number B and of the exponent n produces a reduction of the amplitude of the plug, see Figs. 6-9. The same occurs in the case of a diverging channel ii), see Figs. 10-13. The non-monotonic case iii) is studied assuming a sinusoidal wall function, see Figs. 14-17. In this case the increase of B and n results in a reduction of the plug amplitude when the channel is expanding and in an expansion of the plug amplitude when the channel is narrowing. The cross sections corresponding to $h_x = 0$ are such that $v = \sigma_x = 0$, as expected.

Channel profile	Q	B	n	z_o	Figure
$h(x) = 0.9 + 0.1\sin(2\pi x)$	0.72	5	0.5	0.36	Fig. 10, 11
$h(x) = 0.9 + 0.1\sin(2\pi x)$	0.79	15	2	0.11	Fig. 12, 13

Table 3: Case iii) Non monotonic channel.

5. Numerical simulations with non constant viscosity and yield stress

We now perform some numerical simulations for the case with non constant rheological parameters, Figs. 18, 19, 20. In particular we shall assume that

$$\tau_y = e^{\beta p}, \qquad \mu = e^{\alpha p},$$

so that

$$g(p) = e^{(\beta-\alpha)p}, \qquad \frac{dg}{dp} = (\beta - \alpha)g(p).$$

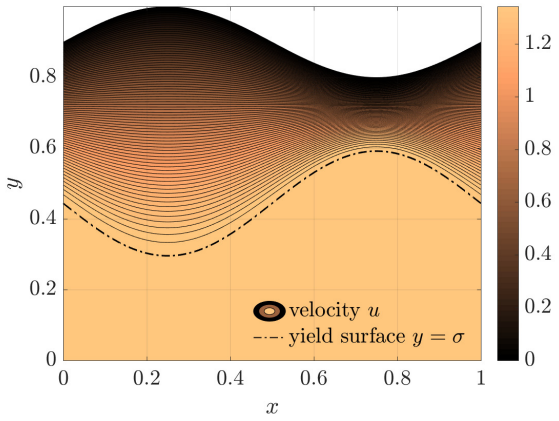

Figure 14: Case iii) $n = 0.5$. Velocity component u.

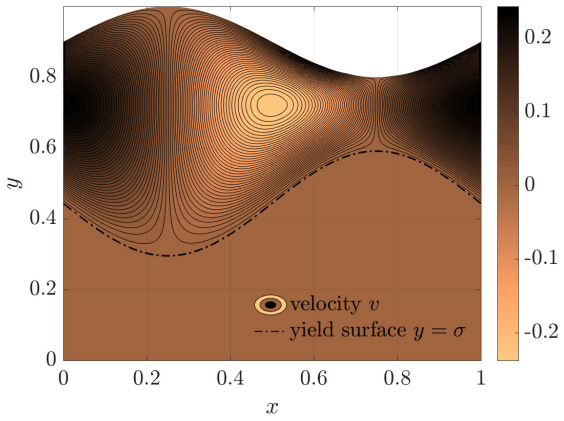

Figure 15: Case iii) $n = 0.5$. Velocity component v.

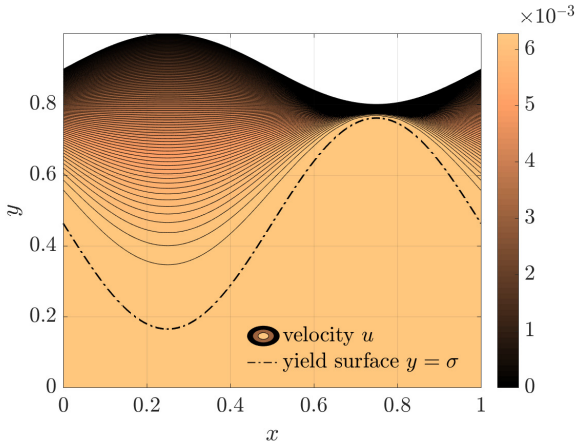

Figure 16: Case iii) $n = 2.5$. Velocity component u.

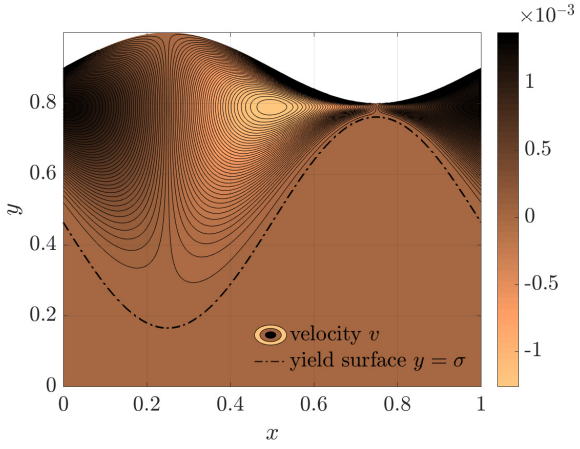

Figure 17: Case iii) $n = 2.5$. Velocity component v.

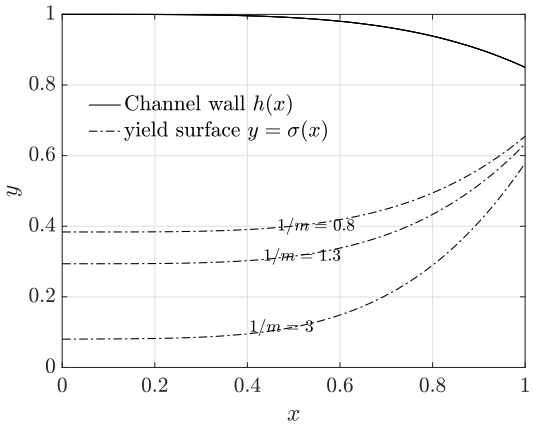

Figure 18: Non constant viscosity and yield stress.

Notice that the assumption $\mu = e^{\alpha p}$ corresponds to the Barus formula for the viscosity [1]. We consider a converging channel of the form

$$h(x) = 1 - 0.15x^4.$$

We begin by studying the dependence of the yield surface on the parameter n, see Fig. 18. In this case we consider the set of data shown in Table 4, As one can

Channel profile	Q	B	α	β
$h(x) = 1 - 0.15x^4$	0.83	5	1	0.5

Table 4: Non constant viscosity and yield stress. Fig. 18

see the plug reduces its amplitude as n increases. Then we study the dependence on the parameter α. In this case we use the values of the Table 5. Looking

Channel profile	Q	B	n	β
$h(x) = 1 - 0.15x^4$	0.81	15	3	0.5

Table 5: Non constant viscosity and yield stress. Fig. 19

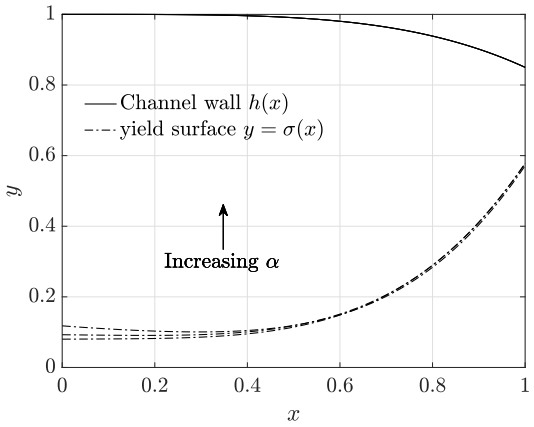

Figure 19: Non constant viscosity and yield stress.

at Fig. 19, we notice that the plug becomes narrower as α increases. Finally we consider the dependence on β using the parameters of Table 6, see Fig. 20. In this case the increase of β produces an increase of the plug amplitude. An

Channel profile	Q	B	n	α
$h(x) = 1 - 0.15x^4$	0.83	15	3	1

Table 6: Non constant viscosity and yield stress. Fig. 20

interesting feature that we observe is that, differently from the case of constant rheological parameter, here the monotonicity of the yield surface and of the wall function are not necessarily opposite. This property is clearly visible in Fig. 19This is in contrast with all the models with constant viscosity and yield stress applied to various types of visco-plastic flows, see [16], [7], [8], [9].

[1] C. Barus, *Isothermals, isopiestics and isometrics relative to viscosity*, Amer. J. Sci., 45, (1893), 27–96.

[2] E.C. Bingham, Fluidity and Plasticity, McGraw-Hill, New York, (1922).

[3] N. Casson, *A Flow Equation for Pigment-Oil Suspensions of the Printing Ink*

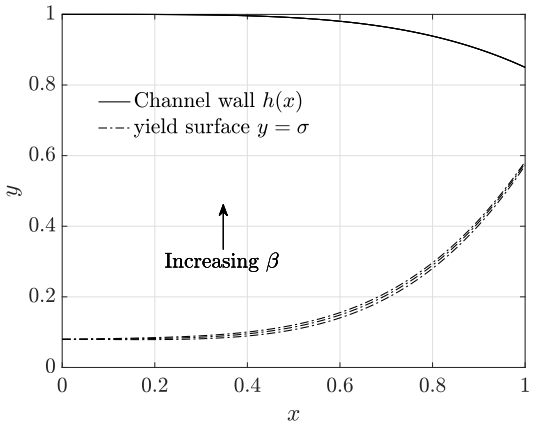

Figure 20: Non constant viscosity and yield stress.

Type, In C. C. Mill, Ed., Rheology of Disperse Systems, Pergamon Press, Oxford, (1959), 84–104.

[4] A. Fincke, *Beitrage zur Losung rheologischer Probleme in der Schokoladentechnologie*, Dissertation, TH Karlsruhe (1961).

[5] I.A Frigaard, S.D. Howison, I.J. Sobey, *On the stability of Poiseuille flow of a Bingham fluid*, J. Fluid Mech., 263, (1994), 133–150.

[6] I.A. Frigaard, D.P. Ryan, Flow of a visco-plastic fluid in a channel of slowly varying width, J. Non-Newtonian Fluid Mech. 123, (2004), 67-83.

[7] L. Fusi, A. Farina, F. Rosso, S. Roscani, *Pressure driven lubrication flow of a Bingham fluid in a channel: A novel approach*, Journal of Non-Newtonian Fluid Mechanics, 221, (2015), 66–75.

[8] L. Fusi, A. Farina, F. Rosso, *Planar squeeze flow of a Bingham fluid*, Journal of Non-Newtonian Fluid Mechanics, 225, (2015), 1–9.

[9] L. Fusi, A. Farina, *Peristaltic flow of a Bingham fluid in a channel*, International Journal of Non-Linear Mechanics, 97, (2017), 78–88.

[10] L. Fusi, F. Rosso, *Creeping flow of a Herschel-Bulkley fluid with pressure-dependent material moduli*, European Journal of Applied Mathematics, 29, (2018), 352–368.

[11] L. Fusi, *Channel flow of viscoplastic fluids with pressure-dependent rheological parameters*, Physics of Fluids, 30, (2018), 073102.

[12] W.H. Herschel, R. Bulkley, *Konsistenzmessungen von Gummi-Benzollosungen*, Kolloid-Zeitschrift, 39, (1926), 291–300.

[13] R. Huilgol, *Fluid mechanics of viscoplasticity*, Springer–Verlag Berlin Heidelberg, (2015).

[14] L. Muravleva, *Squeeze plane flow of viscoplastic Bingham material*, Journal of Non-Newtonian Fluid Mechanics, 220, (2015), 148–161.

[15] L. Muravleva, *Axisymmetric squeeze flow of a Casson medium*, Journal of Non-Newtonian Fluid Mechanics, 267, (2019), 35–50.

[16] P. Panaseti, G.C. Georgiou, I. Ioannou, *Lubrication solution of the flow of a Herschel-Bulkley fluid with pressure-dependent rheological parameters in an asymmetric channel* Physics of Fluids 31, 023106 (2019).

[17] A. Putz, I.A. Frigaard, D.M. Martinez, *On the lubrication paradox and the use of regularization methods for lubrication flows*, J. Non-Newtonian Fluid Mech. 163, (2009), 62–77.

[18] G.W. Scott Blair, J.C. Hening, A. Wagstaff, *The flow of cream through narrow glass tubes*, J. Phys. Chem., 43, (1939), 853–864.